MAUSAM, **71**, 1 (January 2020), 1-10

551.501.86

Comparison of GNSS and INSAT-3D sounder retrieved precipitable water vapour and validation with the GPS Sonde data over Indian Subcontinent

RAMASHRAY YADAV, N. PUVIARASAN*, R. K. GIRI, C. S. TOMAR and VIRENDRA SINGH

India Meteorological Department, New Delhi – 110 003, India

**India Meteorological Department, Chennai – 600 006, India*

(*Received 1 May 2019, Accepted 16 September 2019*)

e mail : ramashray.5329@gmail.com

सार – वायुमंडलीय प्रक्रियाओं में जलवायु परिवर्तन से लेकर सूक्ष्म मौसम विज्ञान में वर्षणीय जल-वाष्प महत्वपूर्ण भूमिका निभाती है। अंकीय मौसम अनुमान (एन डब्ल्यू पी) मॉडल में वायुमंडल में इसकी स्थिति तथा मूल्यांकन करने के लिए इसका वितरण और मात्रा बता पाना अत्यंत कठिन (क्रांतिक) है। वर्षा के लघु अवधि पूर्वानुमान में त्रुटि का एक बड़ा कारण जलवाष्प के परिशुद्ध तथा अनवरत आँकड़ों की कमी का होना है। वायुमंडलीय जलवाष्प की परिशुद्ध माप का कार्य चुनौती भरा होता है। वायुमंडलीय जलवाष्प के पारंपरिक यथावत मान, जी पी एस सोंडे आर्द्रता संवेदी प्रोफाइल मुख्य रूप से सीमित भू-क्षेत्र से, दिन में 2 बार, सार्वत्रिक समय स्थिरांक (यू टी सी) 0000 तथा 1200 पर उपलब्ध कराए जाते हैं। हाल के वर्षों में भारत मौसम विज्ञान विभाग, इनसैट-3 डी के 19 चैनल के ध्वनित्र (सांउडर) से तीन स्तरों, 1000-900 हेक्टापास्कल, 900-700 हे.पा. तथा 700-300 हे.पा. में वर्षणीय जलवाष्प तथा वायुमंडल के ऊर्ध्वाधर कालम में मेघ रहित स्थिति में, सतह से लगभग 100 हे.पा. तक विस्तार में कुल वर्षणीय जलवाष्प की गणना करता है। आमतौर पर इन आँकड़ों का सत्यापन जी पी एस सोंडे के स्थानिक तथा अस्थायी रूप से रखे गए आँकड़ों द्वारा किया जाता था। प्रस्तुत शोध पत्र में, इनसैट 3-डी उपग्रह से पुन: प्राप्त हुए वर्षणीय जल-वाष्प के आँकड़ों का सत्यापन, भारतीय उपमहाद्वीप पर भू-आधारित वैश्विक पथ-प्रदर्शन उपग्रह प्रणाली (जी एन एस एस) के संजाल (नेटवर्क) से प्राप्त कॉलम एकीकृत वर्षणीय जलवाष्प अनुमानों के साथ किया गया है। भारत में जून, 2017 से मई, 2018 तक की अवधि के जी एन एस एस आँकड़ों की उपयुक्त अनुरूपता के कारण इनसैट 3-डी ध्वनित्र (सांउडर) प्लैटफार्म द्वारा पुन: प्राप्त वर्षणीय जल वाष्प अत्यंत आशाजनक है। इनसैट-3 डी और जी एन एस एस वर्षणीय जलवाष्प के मध्य प्रेक्षित रूट-मीन-स्क्वायर (आर एम एस) 5.4 से 7.1 मि.मी. का अंतर, -4.7 से +2.1 मि.मी. का झुकाव तथा 0.79 से 0.92 का परस्पर गुणांक प्रेक्षित किया गया। जी पी एस सोंडे तथा जी एन एस एस के मध्य परस्पर गुणांक से वर्षणीय जलवाष्प का प्रसार 0.85 से 0.98 आँका गया।

ABSTRACT. Precipitable water vapour (PWV) plays a key role in the atmospheric processes from climate change to micrometeorology. Its distribution and quantity are critical for the description of state and evaluation of the atmosphere in NWP model. Lack of precise and continuous water vapour data is one of the major error sources in short term forecast of precipitation. The task of accurately measuring atmospheric water vapour is challenging. Conventional *in situ* measurements of atmospheric water vapour is provided by GPS Sonde humidity sensors profile twice a day at 0000 and 1200 UTC mainly from limited land regions. In recent years India Meteorological Department (IMD) is computing PWV from 19 channel sounder of INSAT-3D in three layers 1000-900 hPa, 900-700 hPa and 700-300 hPa and total PWV in the vertical column of atmosphere stretching from surface to about 100 hPa under cloud free condition. These data most commonly were validated using spatially and temporally collocated GPS Sonde measurements. In this paper, INSAT-3D satellite retrieved PWV data are validated with column integrated PWV estimates from a network of ground based Global Navigation Satellite System (GNSS) over Indian subcontinent. The PWV retrieved by INSAT-3D sounder platform is very promising, being in a good agreement with the GNSS data recorded over India for the period June, 2017 to May, 2018. The root-mean-square (rms) differences of 5.4 to 7.1 mm, bias of -4.7 to +2.1 mm and correlations coefficient of 0.79 to 0.92 was observed between INSAT-3D and GNSS PWV. The correlations coefficient between GPS Sonde and GNSS derived PWV ranges from 0.85 to 0.98.

Key words – PWV, INSAT-3D, GNSS, GPS Sonde.

1. Introduction

Variability in precipitable water vapour (PWV) directly influences the formation of clouds, atmospheric water transport, energy conversion and its transport over large distances through hydrological cycle. It is meaningful to study spatial and temporal variability of water vapour in the atmosphere. To quantify the amount of water vapour in the atmosphere, the PWV is defined as the height (mm) of the water if all of the water substance

contained in a vertical column of unit horizontal cross section were condensed into liquid. It is also referred to as the total column water vapour. There are two main methods to study the atmospheric PWV; ground based and space based. The important ground based observation methods are GPS radiosonde, sun photometry, ground based Global Navigation Satellite System (GNSS) and microwave radiometry while space based method include COSMIC radio occultation, moderate-resolution imaging spectroradiometer (MODIS), SCIAMACHY, atmospheric infrared sounder (AIRS), INSAT-3D sounder etc. These methods of obtaining PWV information allowed substantial progress in understanding of the processes of water vapour occurring in the lower atmosphere. The radiosonde is considered to be a useful reference tool for atmospheric sounding. The conventional atmosphere sensing techniques such as GPS radiosonde, microwave radiometer and sun photometry have limitations in acquiring the continuous transformation of atmospheric PWV due to their low, inhomogeneous spatial and temporal resolution and high operational costs. The advantages of ground-based GNSS retrievals over conventional PWV retrieval methods are that it provides high precision and high temporal resolution data under all weather conditions at very economical cost (Nilsson and Gradinarsky, 2006; Jin *et al.*, 2007). Space-based satellite sensors provide even wider coverage including the world ocean than regional ground-based networks. Infrared radiances are strongly affected by clouds and because of this satellite retrieval of PWV requires cloud-free conditions. However, the satellite retrieved PWV observations must be inter-compared against reliable measurements in order to assure their quality.

The concept of GNSS meteorology was first introduced by Bevis *et al.* (1992) and PWV data were estimated from Global Positioning System (GPS) observations. As the basis of GNSS meteorology, the electromagnetic signal from a GNSS satellite suffers a delay as it passes across the atmosphere, partially as result of the presence of water vapour. The zenith total delay can be converted into PWV using surface pressure and temperature measurements (Bevis *et al.*, 1994). Remarkable progress has been achieved in recent decades and the accuracy of the GNSS-derived PWV has been proved to be better than 1.5 mm using independent GNSS observations (Duan *et al.*, 1996; Tregoning *et al.*, 1998). Several studies have shown GNSS derived PWV distribution as a useful tool for monitoring severe weather events (Brenot *et al.*, 2006, 2013; Barindelli *et al.*, 2018; Bonafoni and Biondi, 2016; Calori *et al.*, 2016). A number of researchers have studied the variation in atmospheric water vapour in relation with the onset of southwest monsoon and rainfall. Rao *et al.* (2013) have studied the variations in refractivity during southwest Monsoon using GPS radio occultation. They have reported an appreciable increase in the refractivity difference between 600 and 100 hPa well before the arrival of Southwest Monsoon coupled with a dip at the time of onset in conformity with COSMIC GPS RO observations. Puviarasan *et al.* (2015) observed that the time series of PWV estimated from GPS increases to more than 60 mm when Southwest monsoon approaches and sharply decreases on withdrawal at the same location. He also recommended, GPS PWV data is more reliable tool for declaring monsoon arrival and withdrawal than using the satellite (INSAT) derived moisture, particularly over the land region. A dense network of continuously operating ground based GNSS receiver if deployed can accurately provide the progress as well as the activeness of Southwest monsoon on real time. Simon *et al.*, 1994, have studied changes in western Indian Ocean moisture in the middle troposphere, upper troposphere and scale height of water vapour during the period of Monsoon Onset over Kerala (MOK) and the moisture and scale height of water vapour increased about 8 days prior to the onset of Southwest Monsoon over Kerala. Simon *et al.* (2006) observed favourable conditions leading to the MOK using Tropical Rainfall Measuring Mission TRMM/TMI derived total water vapour build up over the Western Arabian Sea by about two and half weeks. Singh *et al.* (2004) observed that amount of PWV over the Arabian Sea and the Indian Ocean is well correlated with onset day of Southwest monsoon over the Indian sub-continent. The maximum value of PWV in the 10-15° N latitude zone is to appear 7-12 days prior to the monsoon onset at Kerala coast. Jade & Vijayan (2008) observed that precise measurements of water vapour over the Himalayas and Tibetan plateau are helpful to investigate the land atmosphere interactions and their effect on the Asian monsoon circulation in terms of driving forces and feedback mechanisms.

The descriptions of retrieval techniques for the three instruments (GNSS, GPS Sonde and satellite) PWV are given in the present work. The objective of the paper is to study the accuracy of the GNSS-derived PWV dataset by comparison with that from GPS Sonde and INSAT-3D sounder retrieved PWV using data for the period June, 2017 to May, 2018.

2. Data and methodology

India Meteorological Department (IMD) established a network of 25 ground based Global Navigation Satellite System (GNSS) receivers collocated with meteorological sensors for continuous monitoring of tropospheric total integrated precipitable water vapour (PWV) for weather events monitoring (Fig. 1). GNSS data were processed using the Trimble Pivot Platform (TPP) software to estimate PWV at every 15 minutes interval. The space and

TABLE 1

GNSS and GPS sonde stations with Latitude, Longitude and Height

S. No.	Station code	Stations name	Latitude	Longitude	Ellipsoid height (m)	GPS sonde model name
1.	JIPR	Jaipur	26.82	75.82	335.37	-
2.	RIPR	Raipur	21.21	81.66	245.56	CF06A
3.	TRVM	Trivandrum	8.51	76.96	-18.44	CF06A
4.	KRKL	Karaikal	10.91	79.84	-79.07	RSG20A
5.	KYKM	Kanyakumari	8.08	77.55	-49.23	-
6.	MPTM	Machilipatnam	16.18	81.15	-61.07	RSG20A
7.	ITNG	Itanagar	27.10	93.83	66.50	-
8.	DMPR	Dimapur	25.88	93.77	114.78	-
9.	DBGH	Dibrugarh	27.48	95.02	55.76	CF06A
10.	JPGI	Jalpaiguri	26.55	88.71	37.41	-
11.	SMLA	Shimla	31.10	77.17	2021.58	-
12.	SRNR	Srinagar	33.97	74.79	1631.64	-
13.	RANI	Ranichori	30.31	78.41	1930.54	-
14.	DWRK	Dwarka	22.24	68.96	-40.12	-
15.	GOPR	Gopalpur	19.30	84.88	-15.94	-
16.	JBPR	Jabalpur	23.10	79.99	355.09	-
17.	GRPP	Gorakhpur	26.74	83.43	22.19	-
18.	SGGN	Sri Ganga Nagar	29.92	73.89	132.17	-
19.	DELH	Delhi	28.59	77.22	165.06	DFM09
20.	PUNE	Pune	18.54	73.84	487.72	-
21.	BHPL	Bhopal	23.24	77.42	476.22	-
22.	NGPR	Nagpur	21.09	79.06	253.57	DFM09
23.	BWNR	Bhubaneshwar	20.25	85.82	-16.72	RSG20A
24.	PNJM	Panjim	15.49	73.83	-23.04	CF06A
25.	ARGD	Aurangabad	19.87	75.39	528.13	-

time collocated GNSS derived PWV data have been compared with INSAT-3D derived total PWV. The space and time collocated GNSS derived PWV data have been also compared with GPS sonde derived PWV at 9 locations (Table 1). To reduce the multipath effects a 5° elevation cut-off angle was fixed. Modified Hopfield the New Mapping functions (NMFs) (Niell, 1996) were used to map the signal path delay from zenith direction to other elevation angels.

2.1. *GNSS Meteorology*

The fundamental observable of GNSS is the signal propagation time from a satellite to a receiver. Multiplying the propagation time by the speed of light in vacuum gives the pseudo range between the satellite and the receiver. The pseudo range is mix of various errors such as clock errors both on receiver and satellite, atmospheric error, multipath error etc. For geodetic applications higher accuracy (millimetre level), carrier phase measurements are necessary because the phase can be measured to 1% of the wavelength of the carrier signal. A carrier phase measurement in units of length can be expressed as:

$$\Theta = D + c(T_r - T_s) - \Delta I + \Delta L + n_\lambda + \varepsilon \quad (1)$$

where, Θ is the carrier phase observable, D is the true distance between the satellite and the receiver; c is the speed of light in vacuum, T_r and T_s are the receiver and satellite clock offsets which can be eliminated by double

Fig. 1. India Meteorological Department Global Navigation Satellite System (GNSS) receiver network

difference techniques. The ionospheric delay ΔI is frequency dependent which can be estimated and removed by forming ionospheric free linear combination using $L1$ and $L2$ carrier phase measurements at two different frequencies.

$$\left[R_{L1} - \frac{f_{L1}^2}{f_{L2}^2}\right]\frac{f_{L1}^2}{f_{L1}^2 - f_{L2}^2} = D + c(T_r - T_s) \tag{2}$$

where,

$$R_{L1} = D + c(T_r - T_s) - \Delta I(f_{L1})$$

$$R_{L2} = D + c(T_r - T_s) - \Delta I(f_{L2})$$

From equation (2), 99.9% of ionospheric delay is calculated accurately and can be eliminated.

ΔL, the total delay is sum of zenith hydrostatic delay and zenith wet delay given by (Bevis *et al.*, 1992; Bevis *et al.*, 1994; Davis *et al.*, 1985) in the neutral atmosphere given by:

$$\Delta L = 10^{-6}\int N(s)ds \tag{3}$$

$$\Delta L = \Delta L_h^0 + \Delta L_w^0 \tag{4}$$

The zenith hydrostatic delay (ZHD) in mm can be estimated by measuring surface pressure P_s (in hPa) as follows:

$$\Delta L_h^0 = \text{ZHD} = (2.2779 \pm 0.0024)\, p_s / f(\phi, H) \tag{5}$$

$$f(\phi, H) = 1.00266\cos 2\phi - 0.00028H \tag{6}$$

where, f (ϕ, H) accounts for the variation in gravitational acceleration with latitude ϕ and the height H of the surface above the ellipsoid (in kilometres). The ZWD is obtained by subtracting the ZHD from ZTD, the PWV (mm) estimates were then derived by scaling the ZWD with the multiplication factor Π is given by:

$$PW = \Pi * \text{ZWD} \tag{7}$$

$$\Pi^{-1} = 10^{-6}\rho R_v[(k_3 / T_m) + k_2] \tag{8}$$

where, ρ is the density of liquid water, R_v is the specific gas constant for water vapour, k_3 and k_2 are physical constant. The water-vapour weighted mean temperature T_m of the atmosphere is defined and approximated as (Wang *et al.*, 2005):

$$T_m \equiv \frac{\int \frac{P_v}{T} dz}{\int \frac{P_v}{T^2} dz}$$

where P_v and T represent vapour pressure and absolute temperature along the zenith path, respectively and the integral intervals are from the earth surface to the atmospheric top. T_m can be obtained from radiosonde vertical profile or from NWP analysis. Assuming a linear relation with surface temperature it is also possible to approximate T_m from station surface temperature (T_s) as follows:

$$T_m = 55.8 + 0.77T_S$$

Error due to T_m : Water vapour weighted vertically averaged mean temperature of the atmosphere T_m is an important parameter of the relationship between PWV and the zenith wet delay as the accuracy of GPS estimates of PWV is directly related to the accuracy of T_m. The water-vapour weighted mean temperature of the atmosphere is defined and approximated as follows:

$$T_m \equiv \frac{\int \frac{P_v}{T} dz}{\int \frac{P_v}{T^2} dz} \approx \frac{\sum_{i=1}^{N} \frac{P_{vi}}{T_i} \Delta Zi}{\sum_{i=1}^{N} \frac{P_{vi}}{T_i^2} \Delta Zi}$$

T_m is function of vertical profile of atmospheric temperature and humidity. Using equations, the relative error of PW due to errors in T_m is given by

$$\frac{\Delta PW}{PW} = \frac{\Delta \Pi}{\Pi} = \frac{1}{1+\frac{k_2}{k_3}T_m} * \frac{\Delta T_m}{T_m}$$

Since k_2/k_3 is small (~5.9 × $10^{-5}K^{-1}$), the relative error of PWV approximately equals to that of T_m (Bevis *et al.*, 1994). On the basis of above equation, for T_m values 240 K to 300 K, the 1% and 2% accuracies in PWV require errors in T_m less than 2.74 K and 5.48 K on average respectively (Wang *et al.*, 2005).

Mapping functions : In GNSS data processing, the slant path delay is converted to the equivalent ZTD (sum of the ZHD and the ZWD) using hydrostatic and wet Mapping Functions (Niell, 1996)

$$\Delta L = m_h(\theta)\Delta L_h^z + m_w(\theta)\Delta L_w^z$$

where, θ is the elevation angle seen from the ground antenna to the satellite.

The remaining term n_λ and ε in equation (1) is integer ambiguity and sum of other unmodelled errors, e.g., signal multipath, antenna phase centre variations and radome effects can be estimated and removed from the long term observations.

2.2. *Precipitable water from GPS Sonde*

Precipitable water vapour content based on GPS Sonde observation can be estimated using the formula of Curry and Webster (1999).

$$\mathrm{PWV} = \frac{1}{g\rho_w}\sum q_i \Delta p$$

where, 'g' is the average gravity acceleration of tropospheric air column, ρ_w is the density of atmospheric water vapour, Δp (hPa) is the difference in pressure between layers and q_i is the discrete specific humidity measured from sonde observation. Three types of GPS sonde are being used in IMD (*i*) DFM-09 GPS sonde (*ii*) CF-06A GPS sonde (*iii*) RSG20A GPS sonde (Table 1). Several factors including dry bias, time lag, calibration error and sensor drift may introduce errors in the PWV estimation from radiosonde data (Miloshevich *et al.*, 2009). It is assumed that measured pressure, temperature and dew-point depression were obtained along a strictly vertical ascent (Niell *et al.*, 2001), although observational evidence suggests that radiosonde ascents are rarely strictly vertical because winds are generally present at all altitudes. Usually, radiosondes are expected to produce PWV with an uncertainty of a few millimeters, which is considered to be the accuracy standard of PWV for meteorologists (Niell *et al.*, 2001).

TABLE 2

INSAT-3D sounder channel specification

Channels	Spectral range micron	Resolution
VISIBLE(1)	0.67-0.72	10 × 10 km
SWIR(6)	3.67-4.59	10 × 10 km
MWIR(5)	6.38-11.33	10 × 10 km
LWIR(7)	11.66-14.85	10 × 10 km

2.3. *Precipitable water vapour from INSAT-3D sounder*

Sounding system of the satellite provides vertical profiles of temperature (40 levels from surface to ~70 km), humidity (21 levels from surface to ~15 km) and integrated ozone from surface to top of the atmosphere. Vertical profiles of temperature and moisture can be derived from radiances in 19 channels, using the first guess from NWP data. INSAT-3D sounder channels brightness temperature values are averaged over a number of field of view (FOVs) prior to application of retrieval algorithm. Based on this, retrieval algorithm has option for retrieving the vertical profiles at 30 km (3 × 3 pixels) and 10 km resolution (each pixel). The Sounder has eighteen narrow spectral channels in shortwave infrared, middle infrared and long wave infrared regions and one channel in the visible region. The ground resolution at nadir is 10 × 10 km for all nineteen channels. Specifications of sounder channels are given in Table 2.

As INSAT-3D PWV is sensitive to the presence of clouds in the field of view (limitation of Infra-red sounder sensors), hence the PWV values collected under clear sky conditions were used in this study. Atmospheric profile retrieval algorithm for INSAT-3D Sounder is a two-step approach. The first step includes generation of accurate hybrid first guess profiles using combination of statistical regression retrieved profiles and model forecast profiles. The second step is nonlinear physical retrieval to improve the resulting first guess profile using Newtonian iterative method. The retrievals are performed using clear sky radiances measured by sounder within a 3 × 3 field of view (approximately 30 × 30 km resolution) over land for both day and night (INSAT-3D ATBD, 2015). The GNSS and INSAT-3D retrieved PWV values are matched at every hour. Four sets of regression coefficients are

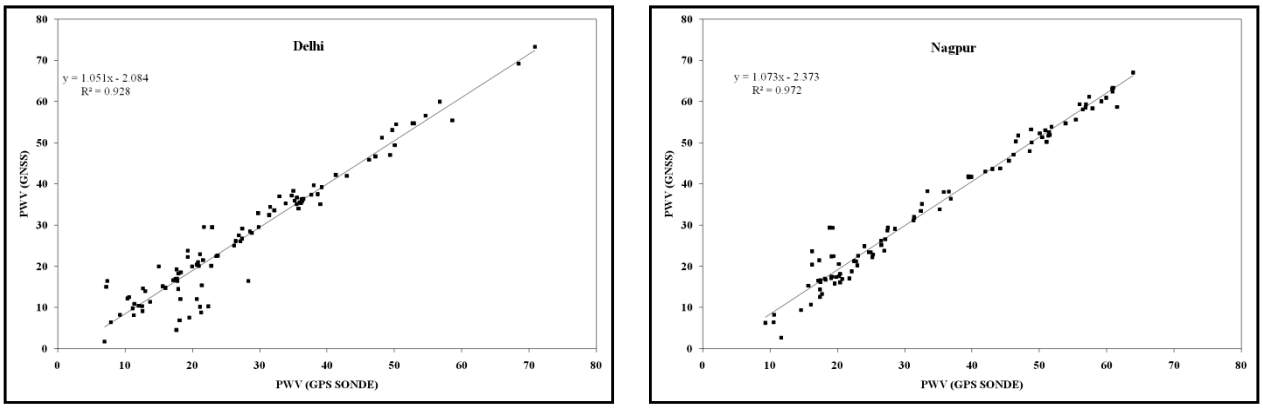

Fig. 2. Scatterplots of GNSS and GPS sonde PWV (DFM-09 GPS sonde). The correlation coefficient (R) is 96% for Delhi and 98% for Nagpur

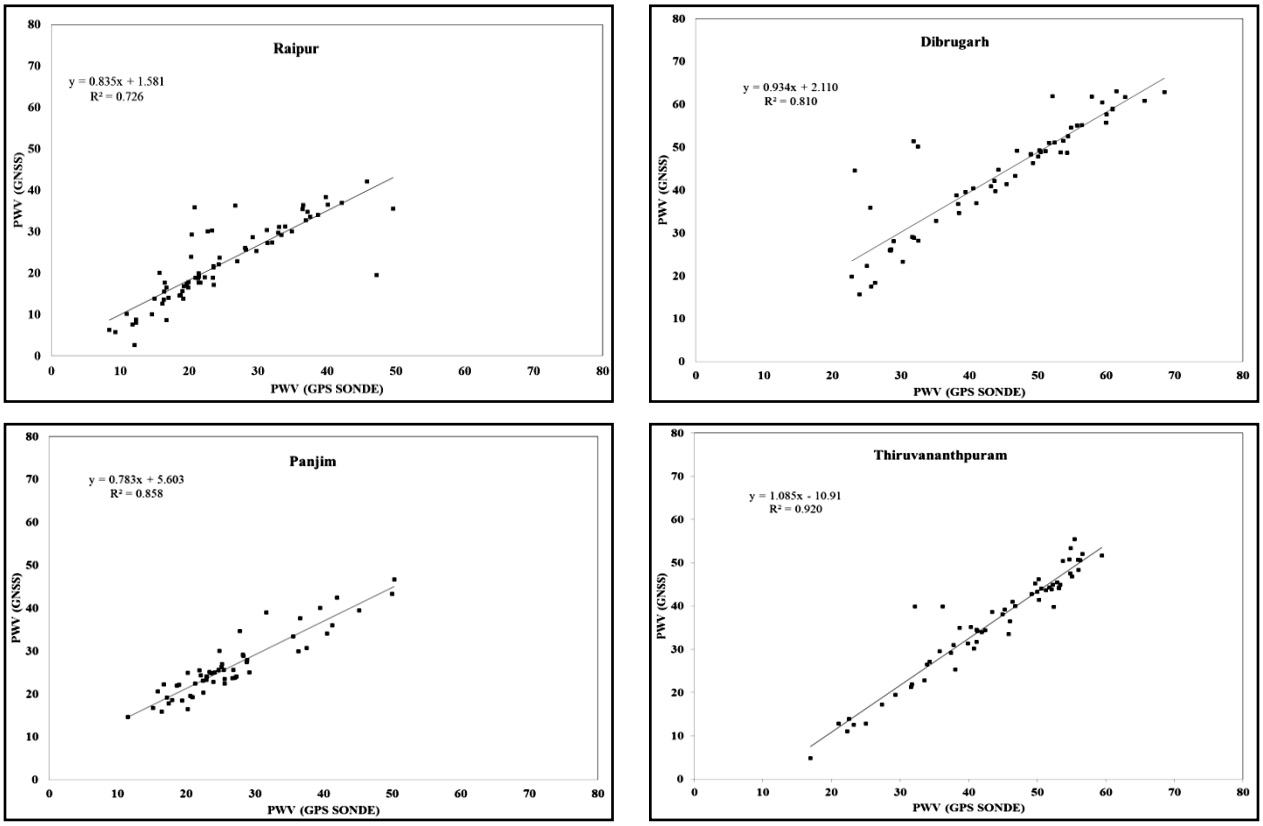

Fig. 3. Scatterplots of GNSS PWV data validated with GPS sonde (CF06A)

generated, two sets for land and ocean daytime conditions and the other two sets for land and ocean night-time conditions using a training dataset comprising historical radiosonde observations representing atmospheric conditions over INSAT-3D observation region. Precipitable Water Vapour in mm can be given as:

$$\text{PWV} = \int_{p_1}^{p_2} \frac{q}{g\rho_w} dp$$

where, 'g' is the acceleration of gravity, p_1 = surface pressure, p_2 = top of atmosphere pressure (*i.e.*, about 100 hPa beyond which water vapour amount is assumed to be in negligible). Unit of precipitable water is mm depth of equal amount of liquid water above a surface of one square meter. IMD is computing PWV from 19 channel sounder of INSAT-3D in three layers *i.e.*, 1000-900 hPa, 900-700 hPa, 700-300 hPa and total PWV in the vertical column of atmosphere stretching from surface to about 100 hPa during cloud free condition. Monsoon, severe

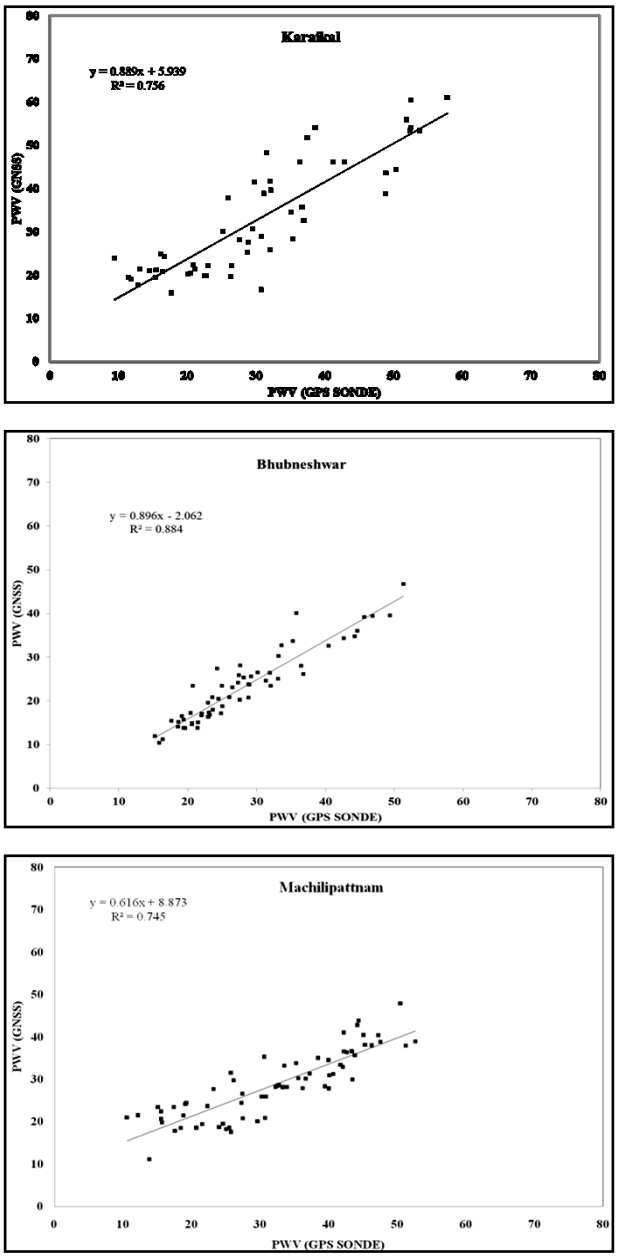

Fig. 4. Scatterplots of GNSS and GPS Sonde (RSG20A) PWV

weather, cloudy condition puts the limitation for sounder profile (Venkat Ratnam *et al.*, 2016).

3. Results and discussion

3.1. *Validation of PWV derived from ground based GNSS with GPS sonde*

To evaluate the accuracy of the GNSS retrieved PWV across mainland India, the comparison are carried out with GPS sonde derived PWV using collocated 9 stations from June, 2017 to May, 2018. The GNSS and GPS Sonde data were matched at 0000 UTC at nine stations for comparison. Correlation coefficient (R), bias and root mean square (rms) differences are presented in Figs. (2-4) and Table 3. The correlation coefficients of GNSS stations Delhi and Nagpur is 0.96 and 0.98. The lower correlation Coefficient in Delhi may be attributed due to the distance between GPS Sonde site which is about 18 km away from GNSS site and Nagpur GPS Sonde and GNSS sites are collocated. The Correlation coefficient of Raipur, Dibrugarh and Panjim are 0.85, 0.90 and 0.92 respectively. The Correlation coefficient of Karaikal, Bhubneshwar, Thiruvananthapuram and Machilipattnam are 0.86, 0.94, 0.96 and 0.86. Both Karaikal and Machilipattnam are coastal stations. The bias between the GPS Sonde and GNSS values of PWV (Table 3) is less than 4 mm except for Thiruvananthapuram (7.2 mm) and Bhubneshwar (4.94 mm). RMS differences between GPS Sonde and GNSS values of PWV are approximately less than 5 mm (Table 3). The relatively larger PWV difference is observed at the coastal stations of India.

TABLE 3

Validation of GNSS PWV with GPS Sonde PWV. [Correlation coefficient (R), Bias and Root mean square error (RMSE) between GNSS PWV with GPS Sonde PWV]

Station	R	Bias	RMSE
Delhi	0.96	-0.48	3.77
Nagpur	0.98	-0.1	1.42
Panjim	0.92	0.15	2.59
Raipur	0.85	2.50	3.67
Dibrugarh	0.90	0.80	2.35
Karaikal	0.86	-2.58	4.50
Machilipattnam	0.86	3.44	4.94
Thiruvananthpuram	0.96	7.20	5.05
Bhubneshwar	0.94	4.94	4.33

3.2. *Comparison of PWV derived from ground based GNSS with INSAT-3D sounder*

Comparison of PWV derived from GNSS and INSAT-3D under clear sky conditions was analysed for the period June, 2017 to May, 2018. The number of observations (N), Root Mean Square Error (RMSE), Correlation Coefficient (R) and bias of each GNSS and INSAT-3D stations are given in Table 4. The RMSE ranges from 5.41 to 7.14 mm. The bias between GNSS and INSAT-3D sounder values of PWV is less than 1 mm except for New Delhi (1.92 mm) and Jalpaiguri (2.14 mm). Fig. 5 shows Taylor diagram for different stations which provides standard deviation, correlation coefficient and RMS error between observed GNSS and

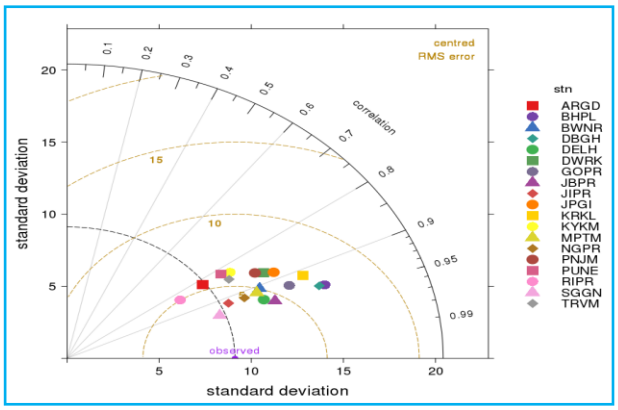

Fig. 5. Taylor diagram for GNSS PWV *versus* INSAT-3D sounder derived PWV at different stations

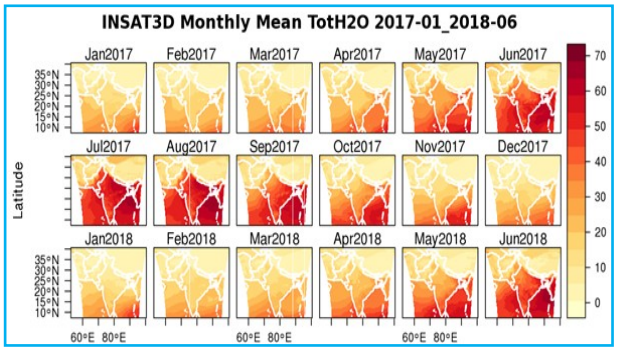

Fig. 6. Monthly mean of PWV (mm) derived from INSAT-3D sounder

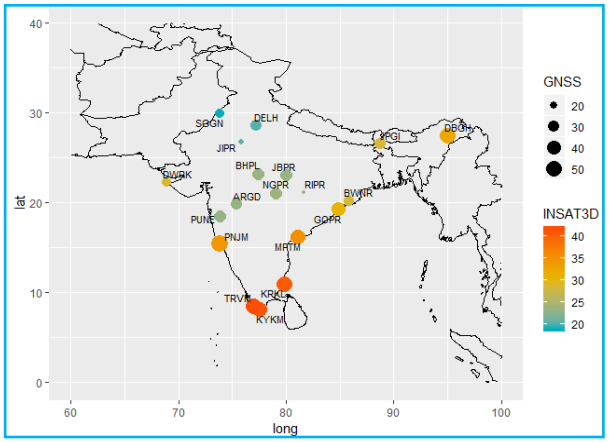

Fig. 7. Spatial view of annual mean PWV (mm) derived from GNSS and INSAT-3D sounder derived

INSAT-3D retrieved PWV. The standard deviation in the Taylor diagram shows the variability between GNSS and INSAT-3D retrieved PWV.

3.3. *Distribution and variability of PWV*

The PWV values depict strong seasonality; reaches maximum in monsoon season and minimum in the winter season. Fig. 6 provides the month-wise spatial distribution of INSAT-3D retrieved PWV. The PWV values are higher during June, July, August and September compared to other months under clear sky condition. The lowest values of PWV are observed during January month over the northwest and central parts of the country, increasing eastwards. The similar winter pattern continues during February and March but with slightly higher values. With the onset of the pre-monsoon season in April, PWV shows a general increase over the whole country. Local terrain effects are responsible for the pockets of the higher or lower values seen in the PWV distribution. A similar PWV distribution is observed in May but with relatively higher values over the entire country. The values of PWV over India further increases with the onset of the monsoon in June with higher values occurring over north-east India. When the monsoon approaches to the stations, PWV increases further and reaches to an average value of 55 mm or more. During July and August, whole country except extreme north has uniformly high values of PWV. The PWV values fall over the country as the withdrawal of the monsoon starts in September. There is a uniform fall of PWV values over the whole country from September to October. November is a transition month from post-monsoon to winter season and December shows the distribution similar to normal winter pattern.

Fig. 7 presents the spatial distribution of GNSS derived annual mean PWV for the period June, 2017 to

TABLE 4

Comparison of GNSS-PWV and INSAT-3D-PWV

Station Name	N	RMSE	R	Bias
Aurangabad	2346	5.56	0.79	0.74
Bhopal	874	5.56	0.87	-0.58
Bhubaneshwar	1357	6.40	0.88	-0.92
Dibrugarh	1069	6.44	0.92	0.39
Dwarka	2294	6.86	0.90	-4.19
Gopalpur	3332	5.91	0.87	-0.86
Jabalpur	561	6.42	0.86	-4.72
Jaipur	869	5.93	0.87	-1.38
Jalpaiguri	1541	7.14	0.87	2.14
Kanyakumari	1542	5.77	0.91	-2.59
Karaikal	1112	5.67	0.92	-1.68
Machilipattnam	1517	6.08	0.86	-3.01
Nagpur	1989	5.51	0.84	-0.51
New Delhi	1978	5.53	0.88	1.92
Panjim	1962	5.64	0.86	-0.49
Pune	478	5.96	0.86	-0.04
Shimla	808	5.51	0.81	-1.51
Thiruvananthpuram	916	5.41	0.88	0.65

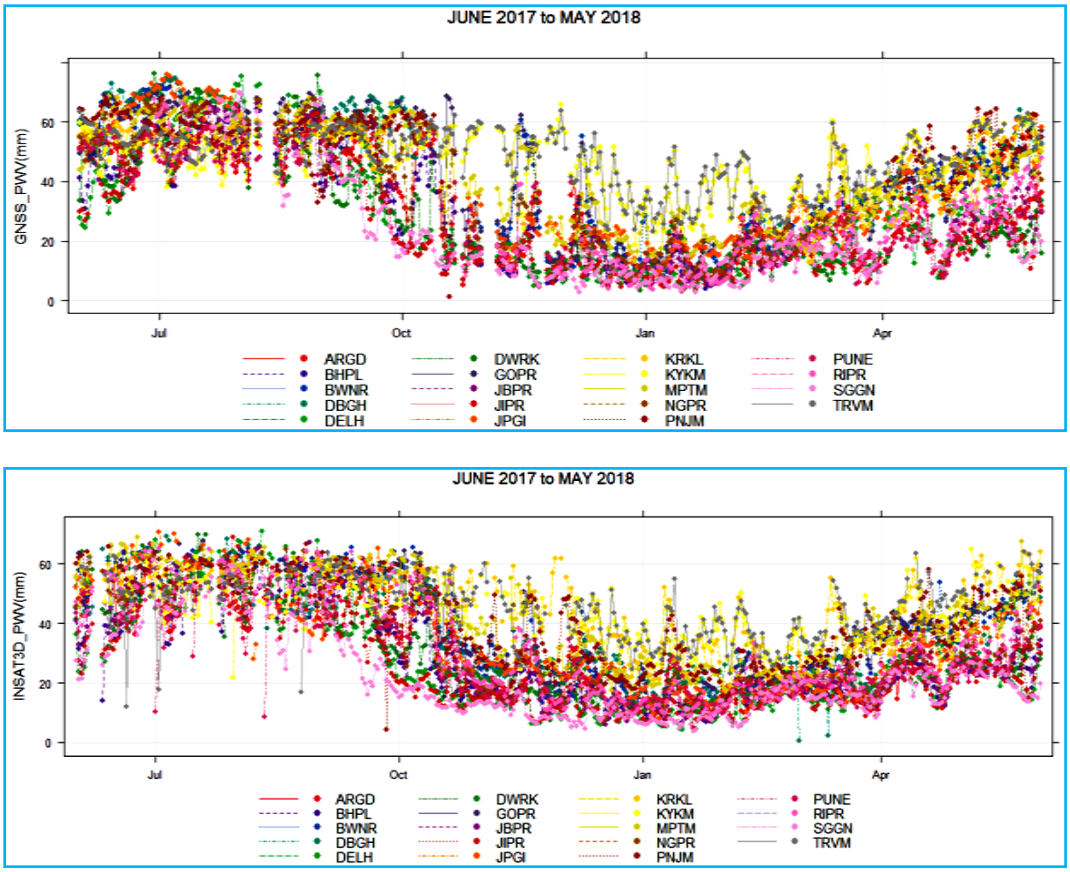

Fig. 8. Time series plot of daily average PWV derived from GNSS and INSAT-3D sounder for the period June, 2017 to May, 2018

May, 2018. The PWV value is largest in the coastal region of India due to sufficient moisture supply from the sea throughout the year. The annual mean values of PWV ranges from 43.4 to 54.7 mm at coastal sites. The PWV value is also high in north-east India. The lowest value of PWV of order less than 30 mm occurred over North India. The time series of the PWV values derived using GNSS and INSAT-3D sounder is given in Fig. 8. The annual variation of PWV based on seasons is clearly seen at all the stations with a peak during the monsoon season.

4. Conclusions

The present study has been carried out for GNSS stations of India Meteorological Department for the period of June, 2017 to May, 2018. The comparison of PWV retrieved from GNSS and GPS Sonde reveal the correlation coefficient varying from 0.98 at Nagpur and 0.85 at Raipur. The bias between the GPS Sonde and GNSS values of PWV is less than 4 mm except for Thiruvananthapuram and Bhubaneswar. The root mean square error between GPS Sonde and GNSS values of PWV are less than 5 mm at almost all the stations. The relatively larger PWV difference is observed at the coastal stations of India. The comparison of PWV retrieved from GNSS and INSAT-3D sounder exhibit a root mean square error ranging from 5.41 to 7.14 mm and a correlation above 0.79. The PWV distribution from GNSS stations across mainland India is also analysed. It was found that the largest PWV value occurs in the coastal region of India and in general PWV value shows a decreasing trend from south to north and increasing trend from west to east.

The comparison of PWV time series derived from GNSS with that from GPS sonde and INSAT-3D sounder data shows that the accuracy of the calculated PWV values is high. India is an ideal place for investigation of regional PWV responses to the climate change. The ground-based GNSS derived PWV will become an important independent data source in climate monitoring as the length of the time series grows. The GNSS-derived PWV value can be useful for investigation of weather forecasting and nowcasting in particular, precipitation forecasting. The simulation experiments should be carried out to assess the quality improvement of weather forecasts when GNSS derived

PWV data are incorporated in models in order to fruitfully exploit the potential possibilities.

Acknowledgements

The authors would like to thank Director General of Meteorology (DGM), New Delhi, for his continuous encouragement and providing all the facilities to carry out this research work. Authors also gratefully acknowledge the help rendered by Dr. V. K. Soni in discussion and analysis.

The contents and views expressed in this research paper/article are the views of the authors and do not necessarily reflect the views of the organizations they belong to.

References

Barindelli, S., Realini, E., Venuti, G., Fermi, A. and Gatti, A., 2018, "Detection of water vapor time variations associated with heavy rain in northern Italy by geodetic and low-cost GNSS receivers", *Earth Planets Space*, **70**, 28, https://doi.org/10.1186/s40623-018-0795-7.

Bevis, M., Businger, S. and Chiswell, S., 1994, "GPS meteorology: Mapping zenith wet delays on to precipitable water", *J. Appl. Meteorology*, **33**, 379-386.

Bevis, M., Businger, S., Herring, T. A., Rocken, C., Anthes, R. A. and Ware, R., 1992, "GPS Meteorology: Remote sensing of atmospheric water vapor using the Global Positioning System", *J. Geophysics. Res.*, **97**, D14, 15787-15801.

Bonafoni, S. and Biondi, R., 2016, "The usefulness of the global navigation satellite systems (GNSS) in the analysis of precipitation events", *Atmos. Res.*, **167**, 15-23.

Brenot, H., Ducrocq, V., Walpersdorf, A., Champollion, C. and Caumont, O., 2006, "GPS zenith delay sensitivity evaluated from high-resolution numerical weather prediction simulations of the 8-9 September, 2002 flash flood over southeastern France", *J. Geophys. Res.*, **111**, D15105, http://dx.doi.org/10.1029/2004JD005726.

Brenot, H., Neméghaire, J., Delobbe, L., Clerbaux, N., De Meutter, P., Deckmyn, A., Delcloo, A., Frappez, L. and Van Roozendael, M., 2013, "Preliminary signs of the initiation of deep convection by GNSS", *Atmos. Chem. Phys.*, **13**, 5425-5449, http://dx.doi.org/10.5194/acp-13-5425-2013.

Calori, A., Santos, J., Blanco, M., Pessano, H., Llamedo, P., Alexander, P. and de la Torre, A., 2016, "Ground-based GNSS network and integrated water vapor mapping during the development of severe storms at the Cuyo region (Argentina)", *Atmos. Res.*, **176**, 267-275.

Curry, J. H. and Webster, P. J., 1999, "Thermodynamics of Atmosphere and Oceans", p471, Academic Press.

Davis, J. L., Herring, T. A., Shapiro, I. I., Rogers, A. E. and Elegered, G., 1985, "Geodesy by radio interferometry: Effects of atmospheric modeling errors on estimates of baseline length", *Radio Sci.*, **20**, 1593-1607.

Duan, J., Bevis, M., Fang, P., Bock, Y., Chiswell, S., Businger, S., Rocken, C., Solheim, F., Van Hove, T., Ware, R., McClusky, S., Herring, T. A. and King, R. W., 1996, "GPS meteorology: Direct estimation of the absolute value of precipitable water", *J. Appl. Meteorol.*, **35**, 6, 830-838.

Insat-3D, 2015, "Algorithm Theoretical Basis Document (ATBD)", https://mosdac.gov.in/data/doc/INSAT_3D_ATBD_MAY_2015.pdf.

Jade, S. and Vijayan, M. S. M., 2008, "GPS-based atmospheric precipitable water vapor estimation using meteorological parameters interpolated from NCEP global reanalysis data", *J. Geophys. Res.*, **113**, D03106, doi:10.1029/2007JD008758.

Jin, S. G., Park, J. U., Cho, J. H. and Park, P. H., 2007, "Seasonal variability of GPS-derived zenith tropospheric delay (1994-2006) and climate implications", *J. Geophys. Res. Atmos.*, **112**, D09110, doi:10.1029/2006JD007772.

Miloshevich, L. M., Vomel, H., Whiteman, D. N. and Leblanc, T., 2009, "Accuracy assessment and correction of Vaisala RS92 radiosonde water vapor measurements", *J. Geophys. Res. Atmos.*, **114**, D11305, doi: 10.1029/2008JD011565.

Niell, A. E., 1996, "Global mapping functions for the atmosphere delay at radio wavelengths", *J. Geophys. Res.*, **101**, B2, 3227-3246.

Niell, A. E., Coster, A. J., Solheim, F. S., Mendes, V. B., Toor, P. C., Langley, R. B. and Upham, C. A., 2001, "Comparison of measurements of atmospheric wet delay by radiosonde, water vapor radiometer, GPS and VLBI", *J. Atmos. Oceanic Technol.*, **18**, 830-850.

Nilsson, T. and Gradinarsky, L., 2006, "Water vapor tomography using GPS phase observations: simulation results", *IEEE Trans. Geosci. Rem. Sens.*, **44**, 10, 2927-2941.

Puviarasan, N., Sharma, A. K., Ranalkar, M. and Giri, R. K., 2015, "Onset, advance and withdrawal of southwest monsoon over Indian subcontinent: A study from precipitable water measurement using ground based GPS receivers", *Journal of Atmospheric and Solar-Terrestrial Physics*, **122**, 45-57.

Rao, V. V. M. J., Venkat Ratnam, M., Durga Santhi, Y., Roja Raman, M. and Rajeevan, M., 2013, "On the detection of onset and activity of the Indian summer monsoon using GPS RO refractivity profiles", *Mon. Weather Rev.*, **141**, 2096-2106.

Simon, B. and Joshi, P. C., 1994, "Determination of moisture changes prior to the onset of monsoon over Kerala using NOAA/TOVS satellite data", *Meteorology Atmospheric Physics*, **53**, 223-231.

Simon, B., Rahman, S. H. and Joshi, P. C., 2006, "Conditions leading to the onset of the Indian monsoon: A satellite perspective", *Meteorological Atmospheric Physics*, **93**, 3-4, 201-210, doi:10.1007/s00703-005-0155-6.

Singh, R. P., Dey, S., Sahoo, A. K. and Kafatos, M., 2004, "Retrieval of water vapor using SSM/I and its relation with the onset of monsoon", *Annales Geophysicae*, **22**, 8, 3079-3083.

Tregoning, P., Boers, R., O'Brien, D. and Hendy, M., 1998, "Accuracy of absolute precipitable water vapor estimates from GPS observations", *J. Geophys. Res.: Atmosphere*, **103**, D22, 28701-28710.

Venkat Ratnam, M., Kumar, A. H. and Jayaraman, A., 2016, "Validation of INSAT-3D sounder data with in situ measurements and other similar satellite observations over India", *Atmos. Meas. Tech.*, **9**, 5735-5745.

Wang, J. H., Zhang, L. Y. and Dai, A. G., 2005, "Global estimates of water-vapor-weighted mean temperature of the atmosphere for GPS applications", *J. Geophysics. Res.*, **110**, D21101.